Impulsive pump-probe and photon-echo spectroscopies of dye molecules in condensed phases

Wayne B. Bosma, Yi Jing Yan, and Shaul Mukamel
Department of Chemistry, University of Rochester, Rochester, New York 14627
(Received 5 July 1990)

A theory for impulsive resonant pump-probe and photon-echo spectroscopies of polyatomic dyes in solution is developed. A multimode calculation in which the intramolecular and solvation modes are modeled as Brownian oscillators is presented. Electronic dephasing, the time-dependent Stokes shift, and quantum beats are analyzed.

I. THE MULTIMODE BROWNIAN OSCILLATOR MODEL

Femtosecond laser pulses, which are shorter than typical molecular vibrations, make it possible to observe elementary dynamical processes such as a single nuclear vibration in real time.[1-7] The recent 6-fs pump-probe and photon-echo measurements in nile blue and malachite green constitute some remarkable examples of such experiments.[1,2] It is clear that a proper theory which could apply to complex dye molecules in solution requires the introduction of semiclassical methods; the number of relevant vibrational and solvent degrees of freedom is far too large to allow for a completely quantum calculation. In this Brief Report we calculate the pump-probe and photon-echo signal for complex polyatomic molecules. The approach, which is based on calculating the third-order polarization $P^{(3)}$, provides a simple picture for these spectroscopies and an efficient method for numerical computations.

We consider a molecular system consisting of a dye molecule in its solvent environment. We assume that there are only two relevant electronic states: the ground state $|g\rangle$ and the excited state $|e\rangle$; however, we allow for an arbitrary number of solute and solvent modes, which we take to be harmonic. Mode j has fundamental frequency ω_j and we shall denote its dimensionless coordinate by q_j. We assume that the q_j obey the Langevin equation

$$\ddot{q}_j+\gamma_j\dot{q}_j+\omega_j^2 q_j=f_j(t)\ , \tag{1}$$

where $f_j(t)$ is a random Langevin force and γ_j is the friction. We assume the modes to be independent of one another; thus, the system's response to the applied radiation fields may be expressed as a product of N response functions corresponding to the N modes.[8] The difference between the excited- and ground-state Hamiltonians is $H_e-H_g\equiv\sum_j U_j$, where $U_j\equiv\omega_j D_j(q_j+D_j/2)$ is the contribution of the jth mode. D_j is the dimensionless displacement between the potential surfaces of electronic excited- and ground-state levels. We next introduce two static quantities representing the first two moments of U_j: $\lambda_j\equiv\langle U_j\rangle=\omega_j D_j^2/2$ and $\Delta_j^2\equiv\langle U_j^2\rangle-\langle U_j\rangle^2=\lambda_j\omega_j(2\bar{n}_j+1)$. Here $\langle\ \rangle$ denotes an average over the initial thermal distribution and $\bar{n}_j=[\exp(\hbar\omega_j/k_BT)-1]^{-1}$ is the thermally averaged occupation number of the jth mode. Note that in the high-temperature limit ($k_BT\gg\hbar\omega_j$) we have $\Delta_j^2=2\lambda_j k_BT$.

The linear absorption line shape for this system, in the Condon approximation, may be calculated using a second-order cumulant expansion,[9] resulting in

$$\sigma(\omega)=\mathrm{Re}\int_0^\infty dt\,\exp[i(\omega-\omega_{eg})t]\exp[-g(t)]\ , \tag{2}$$

where ω_{eg} is the molecular 0-0 ground-excited electronic transition frequency (which includes a shift due to interactions with fast solvent electronic degrees of freedom), $g(t)=\sum_j g_j(t)$, and

$$g_j(t)=\frac{1}{2\pi}\int_{-\infty}^{\infty}d\omega\frac{1-\cos\omega t}{\omega^2}C_j(\omega)+\frac{i}{2\pi}\int_{-\infty}^{\infty}d\omega\frac{\sin\omega t-\omega t}{\omega^2}\tanh(\beta\omega/2)C_j(\omega)+i\lambda_j t\ . \tag{3}$$

The spectral density $C_j(\omega)$ is given by

$$C_j(\omega)=\frac{2\Delta_j^2\gamma_j\omega_j^2}{(\omega^2-\omega_j^2)^2+\gamma_j^2\omega^2}\ . \tag{4}$$

The fluctuation-dissipation theorem has been used in calculating the imaginary part of Eq. (3).[9,10]

The cases of which $\gamma_j<2\omega_j$, $\gamma_j=2\omega_j$, and $\gamma_j>2\omega_j$ correspond to the oscillator motion being underdamped, critically damped, and overdamped, respectively. When $\gamma_j\gg2\omega_j$, the oscillator is strongly overdamped, and we get (for $k_BT\gg\hbar\omega_j$)

$$g_j(t)=\frac{\Delta_j^2}{\Lambda_j^2}(\Lambda_j t-1+e^{-\Lambda_j t})+\frac{i\lambda_j}{\Lambda_j}(1-e^{-\Lambda_j t})\ , \tag{5}$$

with $\Lambda_j\equiv\omega_j^2/\gamma_j$. The line-shape function for the stochastic model of spectral line broadening[11] may be obtained by neglecting the imaginary part of Eq. (5); thus the stochastic model does not account for the solvent-induced red shift of fluorescence relative to absorption (the Stokes shift). Inhomogeneous broadening may be incorporated into the calculation by including an overdamped mode with $\Lambda_j=0$.[11,12] For this case, we have $g_j(t)=\frac{1}{2}\Delta_j^2t^2+i\lambda_j t$. For homogeneous broadening, we assume $\Lambda_j/\Delta_j\gg1$, and the line-shape function becomes

$g_j(t)=\hat{\Gamma}_j t$, where $\hat{\Gamma}_j=\Delta_j^2/\Lambda_j$ is the pure dephasing rate. In the following, we shall use the line-shape function $g(t)$ to calculate photon-echo and impulsive pump-probe line shapes.

II. IMPULSIVE PUMP-PROBE SPECTROSCOPY

In a pump-probe experiment, the system is first subjected to a short pump pulse. After a delay τ, a second pulse, the probe, interacts with the system. It is then dispersed in frequency and the probe difference absorption, defined as the probe absorption in the absence of the pump minus the probe absorption in the presence of the pump, is recorded as a function of the detection frequency ω_2 and the delay time τ. In the impulsive limit, the pump and probe pulses are short compared to the dynamical time scales of the solvent and solute nuclear degrees of freedom. The difference absorption signal is then given by[8]

$$S_{\rm PP}(\tau,\omega_2)=\frac{1}{\pi}\mathrm{Re}\int_0^\infty dt\,\exp[i(\omega_2-\omega_{eg})t]\times\{\exp[-g^*(\tau)+2ig''(\tau+t)-2ig''(\tau)]+\exp[-g(t)]\}\ . \tag{6}$$

Here $g''(t)$ denotes the imaginary part of $g(t)$. We may view a pump-probe experiment as a three-step process: preparation, propagation, and detection. First, the pump pulse prepares an initial doorway state by exciting a "particle" into the electronic excited state, leaving a "hole" in the electronic ground state. This particle and hole then propagate, respectively, on the excited- and the ground-state electronic potential surfaces. Finally, after the delay time τ, the doorway state is probed and spectrally resolved. The first and the second terms in the curly brackets of Eq. (6) represent the particle and the hole contributions, respectively.

We have calculated the probe absorption, using Eq. (6), for a four-mode system. The first two modes are high-frequency vibrations with small vibrational relaxations ($\gamma_j<\omega_j$), with fundamental frequencies of 600 and 1500 cm^{-1}. Mode 3 is an overdamped solvation mode, which accounts for line broadening and a time-dependent Stokes shift, which occurs on a 3.5-ps time scale. Mode 4 is an overdamped mode in the inhomogeneous limit ($\Lambda_4=0$). We evaluated Eq. (6) using a standard fast-Fourier-transform routine, with 2048 time points. In Fig. 1(a) we display the spectrum for the first two modes alone. In the figure, we see a peak at the 0-0 frequency, as well as a peak at 1500 cm^{-1}, and peaks at 600 cm^{-1} and its overtone, 1200 cm^{-1}. The overall shape and position of the spectrum do not change with time. Because the pump pulse is short compared to the periods of the underdamped modes, it creates a vibrational coherence in those modes, in the excited electronic state. As a result, the magnitudes of the peaks show a quantum beat oscillation. In Fig. 1(b) we show the spectrum for the full four-mode system. The solvent modes have broadened out the Franck-Condon progressions observed in Fig. 1(a). The peak of the spectrum is now blue shifted and appears to

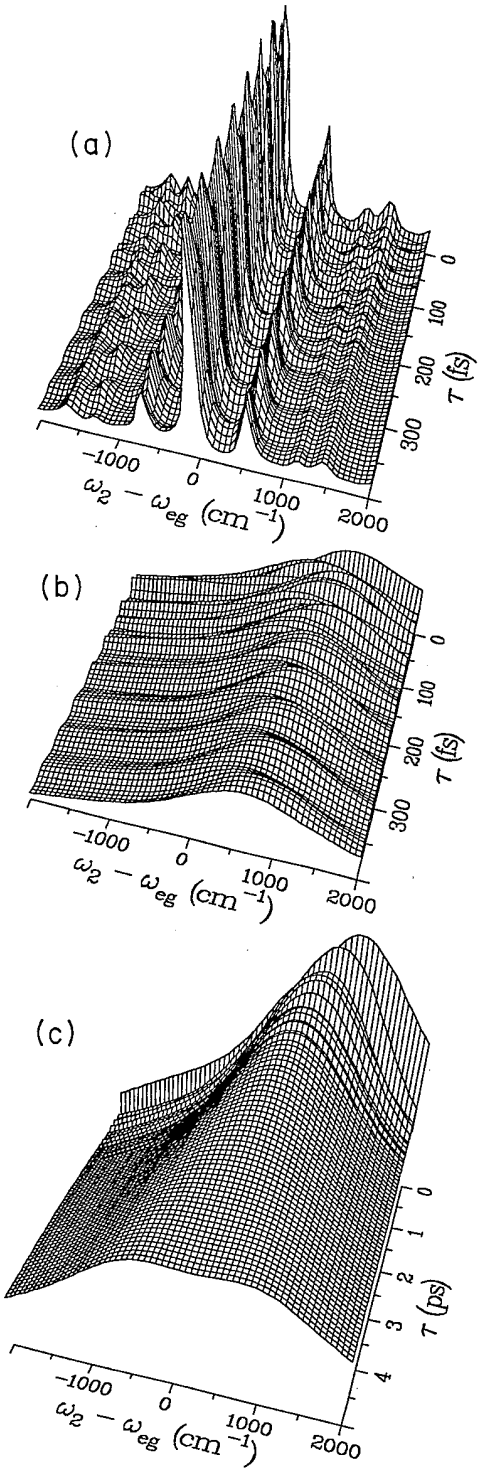

FIG. 1. Time- and frequency-resolved pump-probe differential absorption spectrum. (a) A solute-only calculation for two underdamped modes with fundamental frequencies $\omega_1=600$ cm^{-1} and $\omega_2=1500$ cm^{-1}, displacements $D_1=1.0$ and $D_2=0.8$, and Langevin frictions $\gamma_1=30$ cm^{-1} and $\gamma_2=120$ cm^{-1}. The temperature is 300 K. (b) A four-mode calculation. To the two modes of part (a) we have added an overdamped mode, with relaxation time $\Lambda_3^{-1}=3.5$ ps, reorganization energy $\lambda_3=625$ cm^{-1}, and coupling strength $\Delta_3=510$ cm^{-1}; and an inhomogeneous mode, with $\Delta_4=255$ cm^{-1} and $\lambda_4=155$ cm^{-1}. (c) The calculation of (b) carried out to 5 ps, showing the time-dependent Stokes shift.

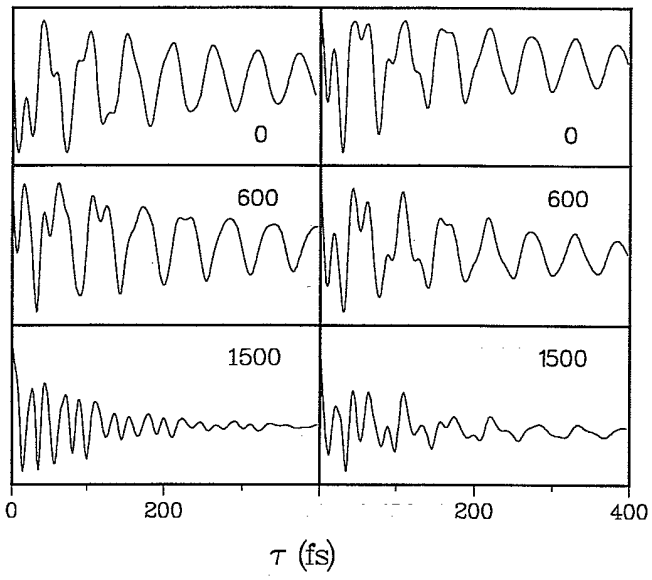

FIG. 2. Time-dependent differential absorption signal for fixed detection frequencies ω_2. The left and right columns correspond to the solute-only [Fig. 1(a)] and four-mode [Fig. 1(b)] calculations of Fig. 1, respectively. In the left column, the detection frequencies are $\omega_2-\omega_{eg}=0$, 600, and 1500 cm^{-1}, as indicated in each panel. In the right column, the detection frequencies are at the absorption maximum ($\omega_2=\omega_{eg}+\lambda_3+\lambda_4$), and 600 and 1500 cm^{-1} to the blue of the absorption maximum, as indicated in the panels. The subplots are on different scales.

oscillate back and forth in frequency as a function of delay time. In Fig. 1(b), the dynamic Stokes shift, which occurs on a 3.5-ps time scale, has not yet begun to occur; hence, the contributions of the two solvent modes are indistinguishable at short times—both seem inhomogeneous on the time scale of the figure. In Fig. 1(c), we extend the calculation of Fig. 1(b) to longer times. The two peaks which appear on the picosecond time scale of Fig. 1(c) correspond to the particle and the hole contributions,[8] and are separated by the Stokes shift due to mode 3.

In Fig. 2, we display slices of the τ-dependent spectra of Figs. 1(a) and 1(b), for frequency values corresponding to the (linear) absorption maximum and 600 and 1500 cm^{-1} to the blue of the maximum. In the left column, which corresponds to Fig. 1(a), we see that the 0- and 600-cm^{-1} slices contain oscillations due to both the 600 and 1500 cm^{-1} modes. The 1500-cm^{-1} slice, however, beats only at the higher frequency. In the right column, we have the two solvent modes in addition to the two high-frequency modes. The solvent's broadening effect on the spectrum has caused the lower-frequency oscillations to become important in the 1500-cm^{-1} slice of the spectrum.

III. IMPULSIVE PHOTON ECHO

In a photon-echo experiment, the molecular system is subjected to two short pulses with wave vectors $\mathbf{k}_1$ and $\mathbf{k}_2$, separated by a delay τ. When the pulses are short compared with the dynamical time scales of the solvent and solute, the photon-echo signal, emitted in the direction $2\mathbf{k}_2-\mathbf{k}_1$ is given by[10,13]

$$S_{\mathrm{PE}}(\tau,t)=\exp[-4g'(t)-4g'(\tau)+2g'(t+\tau)]\ . \qquad (7)$$

Here $g'(t)$ denotes the real part of $g(t)$. The t argument in Eq. (7) refers to the time of detection of the signal. The contribution of an inhomogeneous mode to the spectrum is $S_{\mathrm{PE}}(\tau,t)\sim\exp[-\Delta_j^2(t-\tau)^2]$.

In Fig. 3, we display the photon-echo signal as a function of both t and τ for the four-mode system considered in Sec. II. In the figure, we see an initial decay, followed by oscillations. These are quantum beats, resulting from the modulation of the electronic polarization by vibronic coherences. Because of the inhomogeneous mode, the echo signal is centered at $t=\tau$. The first peak (the free-induction decay) has been cut off to better show the subsequent peaks; it is approximately 50 times as high as is shown in the figure.

For a system characterized by a very large inhomogeneous broadening, the photon-echo signal becomes very sharply peaked at $t=\tau$, and the total signal integrated over t is proportional to $S_{\mathrm{PE}}(\tau,\tau)=\exp[-8g'(\tau)+2g'(2\tau)]$. This relation allows us to better examine the time dependence of the photon-echo decay. For an overdamped (solvent) mode, $g(t)$ is given by Eq. (5). For times short, cf. Λ_j^{-1}, we may expand the real part of Eq. (5) to lowest nonvanishing order, resulting in $S_{\mathrm{PE}}(\tau)\sim\exp[-(\tau/\tau_s)^3]$, with the characteristic short time scale $\tau_s\equiv(4\Delta_j^2\Lambda_j/3)^{-1/3}$. For delay times long, cf. Λ_j^{-1}, the echo decay is proportional to $\exp(-\tau/\tau_l)$, with the characteristic long time scale $\tau_l\equiv\Lambda_j/\Delta_j^2$. These limiting behaviors have been observed experimentally in the gas phase.[14]

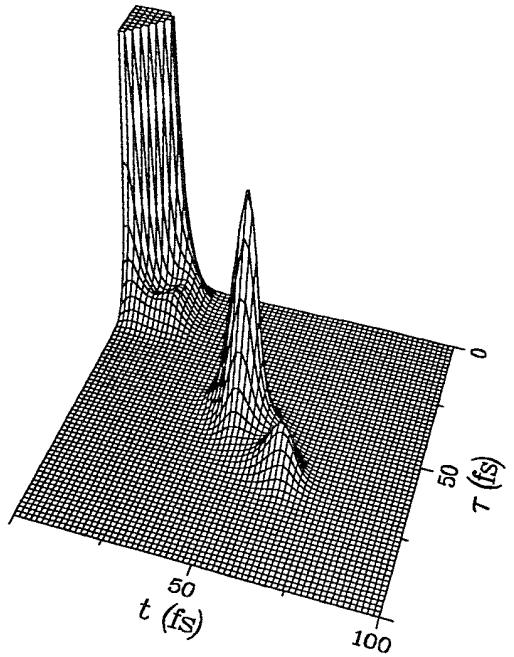

FIG. 3. Photon-echo signal [Eq. (7)], plotted as a function of t and τ, for the four-mode system of Fig. 1(b).

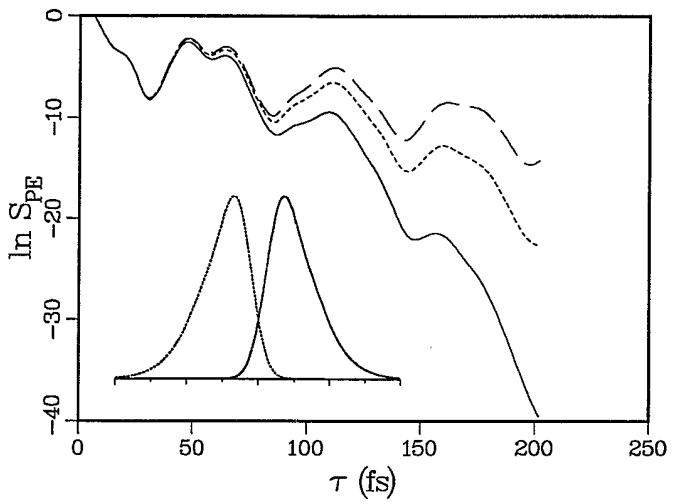

FIG. 4. Solid line: the total photon-echo signal [Eq. (7), integrated over t] for the four-mode system of Fig. 1. In the short-dashed and long-dashed lines the solvent relaxation time of mode 3 (3.5 ps) has been changed to $\Lambda_3^{-1}=10.5$ and 105 ps, respectively. *Inset:* the linear absorption (solid curve) and fluorescence (dotted curve) for this system, which are virtually identical for the three solvent time scales in Fig. 1. The frequency scale is 2000 cm^{-1} between tick marks.

Figure 4 gives the natural logarithm of the total photon-echo signal [Eq. (7), integrated over t] for the four-mode system considered in Sec. II (solid line). The other two curves in Fig. 4 are echo traces for solute-solvent with different values of the solvent-mode correlation time Λ_3^{-1}: The short-dashed line has $\Lambda_3^{-1}=10.5$ ps and the long-dashed line has $\Lambda_3^{-1}=105$ ps. All other parameters are the same as in the solid curve. A larger value of Λ_3^{-1} means that the solvent relaxation of mode 3 is "more homogeneous"; thus we expect that systems with smaller values of Λ_3^{-1} will be characterized by slower echo decays. Corresponding to mode 3 of the three curves in the figure, we have $\tau_s=66$, 95, and 210 fs; this explains the fast initial decay of the curves relative to $\exp(-\Lambda_3\tau)$. It should also be noted that the Langevin friction of the two underdamped modes also contributes a (homogeneous) decay to the curves in Fig. 4. In addition to these decays, the three curves in Fig. 4 exhibit oscillations at the frequencies of the 600- and 1500-cm^{-1} modes. The inset of Fig. 4 gives the absorption (solid line) and fluorescence (dashed line) spectra for the four-mode system. The x axis of the inset corresponds to frequency relative to the 0-0 transition frequency, and runs from -6000 to 6000 cm^{-1}. Unlike the echo signal, these curves do not change appreciably with changing Λ_3, and thus give information only about the total broadening of the system, with no information about the solvent relaxation time scales.

In conclusion, we note that although pump-probe and photon-echo experiments both probe the third-order polarization, they give complementary information regarding the molecular system being studied. The pump-probe experiment gives time-domain information regarding the solute-solvent system while the density matrix for the system is in an electronic population. The homogeneous and inhomogeneous dephasing processes due to the solvent appear as broadenings in the frequency domain, as is the case in the ordinary (linear) absorption and fluorescence line shapes; however, these dephasing processes do not affect the temporal profile of the signal. What we do see in the pump-probe differential absorption signal is vibrational information for the solute modes in the form of quantum beats, and the dynamic Stokes shift, indicative of the solvent's reorientation to stabilize the solute excited electronic state. In the photon-echo experiment, on the other hand, we probe the solute-solvent system while the solute density matrix is in an electronic coherence. As such, we see directly the time scale of the electronic dephasing processes which characterize the solute-solvent system. Furthermore, since the electronic coherence can involve superpositions of vibrational states in the ground- or excited-state electronic manifolds of the solute modes, we see quantum beats due to those modes.

ACKNOWLEDGMENTS

The support of the National Science Foundation, the U. S. Air Force Office of Scientific Research, and the Petroleum Research Fund, administered by the American Chemical Society, is gratefully acknowledged.

[1]P. C. Becker, H. L. Fragnito, J. Y. Bigot, C. H. Brito-Cruz, R. L. Fork, and C. V. Shank, Phys. Rev. Lett. **63**, 505 (1989).
[2]C. H. Brito-Cruz, R. L. Fork, W. H. Knox, and C. V. Shank, Chem. Phys. Lett. **132**, 341 (1986); H. L. Fragnito, J. Y. Bigot, P. C. Becker, and C. V. Shank, *ibid.* **160**, 101 (1989).
[3]P. C. Becker, R. L. Fork, C. H. Brito-Cruz, J. P. Gordon, and C. V. Shank, Phys. Rev. Lett. **60**, 2462 (1988).
[4]M. J. Rosker, F. W. Wise, and C. L. Tang, Phys. Rev. Lett. **57**, 321 (1986); I. A. Walmsley, M. Mitsunaga, and C. L. Tang, Phys. Rev. A **38**, 4681 (1988).
[5]Y. X. Yan and K. A. Nelson, J. Chem. Phys. **87**, 6240 (1987); **87**, 6257 (1987).
[6]J. Chesnoy and A. Mokhtari, Phys. Rev. A **38**, 3566 (1988).
[7]D. McMorrow, W. T. Lotshaw, and G. A. Kenney-Wallace, IEEE J. Quantum Electron. **QE - 24**, 443 (1988).
[8]Y. J. Yan and S. Mukamel, Phys. Rev. A **41**, 6485 (1990).
[9]S. Mukamel, Phys. Rev. A **28**, 3480 (1983); J. Phys. Chem. **89**, 1077 (1985).
[10]Y. J. Yan and S. Mukamel, J. Chem. Phys. (to be published).
[11]R. Kubo, Adv. Chem. Phys. **15**, 101 (1969).
[12]S. Mukamel, Adv. Chem. Phys. **70**, Pt. I, 165 (1988); S. Mukamel, Ann. Rev. Phys. Chem. **41**, 647 (1990).
[13]S. Mukamel, Chem. Phys. Lett. **114**, 426 (1985).
[14]J. Schmidt, P. R. Berman, and R. G. Brewer, Phys. Rev. Lett. **31**, 1103 (1973).